Am J Physiol Cell Physiol 294: C1430–C1435, 2008.
First published April 2, 2008; doi:10.1152/ajpcell.90623.2007.

Surface change of the mammalian lens during accommodation

Aldo C. Zamudio,[1] Oscar A. Candia,[1,2] Chi Wing Kong,[1] Brian Wu,[1] and Rosana Gerometta[1,3]

Departments of [1]Ophthalmology and [2]Structural and Chemical Biology, Mount Sinai School of Medicine, New York, New York; and [3]Oftalmología, Universidad Nacional del Nordeste, Corrientes, Argentina

Submitted 13 December 2007; accepted in final form 2 April 2008

Zamudio AC, Candia OA, Kong CW, Wu B, Gerometta R. Surface change of the mammalian lens during accommodation. *Am J Physiol Cell Physiol* 294: C1430–C1435, 2008. First published April 2, 2008; doi:10.1152/ajpcell.90623.2007.—Classical theories suggest that the surface area of the crystalline lens changes during accommodation while the lens volume remains constant. Our recent work challenged this view by showing that the lens volume decreases as the lens flattens during unaccommodation. In this paper we investigate *1*) the magnitude of changes in the surface of the in vitro isolated cow lens during simulated accommodation, as well as that of human lens models, determined from lateral photographs and the application of the first theorem of Pappus; and *2*) the velocity of the equatorial diameter recovery of prestretched cow and rabbit lenses by using a custom-built software-controlled stretching apparatus synchronized to a digital camera. Our results showed that the in vitro cow lens surface changed in an unexpected manner during accommodation depending on how much tension was applied to flatten the lens. In this case, the anterior surface initially collapsed with a reduction in surface followed by an increase in surface, when the stretching was applied. In the human lens model, the surface increased when the lens unaccommodated. The lens volume always decreases as the lens flattens. An explanation for the unexpected surface change is presented and discussed. Furthermore, we determined that the changes in lens volume, as reflected by the speed of the equatorial diameter recovery in in vitro cow and rabbit lenses during simulated accommodation, occurred within a physiologically relevant time frame (200 ms), implying a rapid movement of fluid to and from the lens during accommodation.

lens surface area calculation; lens volume calculation; lenticular fluid movement; in vitro model for accommodation

THE EYE FORMS CLEAR IMAGES on the retina of objects positioned over a wide range of distances by a process known as accommodation. This is accomplished in higher vertebrates by changes in the shape and surface radii of curvature of the crystalline lens (6, 11). It has been assumed that during this process the volume of the lens remains constant while only its surface changed (13, 14, 24).

In a recent publication, we challenged this classical view of constant volume in the crystalline lens during accommodation (4, 10). Using freshly obtained cow eyes, we isolated the "accommodation system" consisting of the ciliary body, zonulae, and lens. We photographed cow lenses in two accommodative states: in the spontaneous relaxed position and after imposition of a stretching force that increased the lenticular equatorial diameter and reduced the anterior-posterior (A-P) thickness between poles. We also used an analogous approach to calculate the volume of human lenses modeled from data in the literature (2, 3, 9, 12, 21, 22) for 10 and 4 diopter (D) changes in accommodation of 20- and 45-yr-old lenses, respectively (10). As observed with isolated in vitro cow lenses, we calculated that human lenses should lose volume when flatter while accommodative power is reduced. In our previous work, we did not attempt to measure the possible changes in lenticular surface, which has been assumed to occur during accommodation. However, we did suggest that although the lens gets flatter and its volume is reduced, its surface should increase, particularly around its equatorial zone. Moreover, with our previous in vitro experiments on the cow lens, manipulated changes in lens shape were produced with a manual apparatus that required about a minute to exert a force necessary to stretch the lens. Nevertheless, even though we calculated changes in volume in the aforementioned studies, we did not demonstrate that the predicted flow across the surface of the lens could occur during the rapid accommodative changes in lens shape that happen within a time frame of ~200 ms (15).

In this paper we report *1*) the calculated magnitude of changes in the surface of the in vitro isolated cow lens during the accommodation process, as well as that of human lens models, determined from lateral photographs and the application of the first theorem of Pappus; and *2*) the velocity of recovery of the equatorial diameter in prestretched cow and rabbit lenses by using a software-controlled stretching apparatus synchronized to a digital camera. Pappus centroid theorems have been extensively used to determine geometrical dimensions of human eyes, heart ventricles, urinary bladders, and subcellular organelles, to name a few (7, 17, 20, 23). This useful approach allows calculation of volume and surface from two-dimensional images of symmetrical bodies.

From our calculations, we determined that the surface of the human lens model increased with unaccommodation, as expected. However, in the experiments with the cow lenses, the surface decreased in most cases as the lens became flatter during unaccommodation. Only with additional stretching the surface increased. An explanation for this apparent paradox is presented in the DISCUSSION. Furthermore, we were able to indeed show that in vitro cow and rabbit lenses regain their volumes within 200 ms upon the release of a stretching force.

METHODS

Isolation of the Accommodation System in Cows and Rabbits

For all in vitro experiments with bovine lenses, the preparations were dissected and mounted in a similar manner as reported previously (10). Briefly, eyes were obtained immediately upon the death of 3- to 4-yr-old cows (cow life span is around 20 yr) from a slaughterhouse in Argentina and transported to the laboratory at Universidad Nacional del Nordeste. Each eye was dissected from the posterior

Address for reprint requests and other correspondence: O. Candia, Mount Sinai School of Medicine, 100th St. and 5th Ave., New York, NY 10029 (e-mail: oscar.candia@mssm.edu).

The costs of publication of this article were defrayed in part by the payment of page charges. The article must therefore be hereby marked "*advertisement*" in accordance with 18 U.S.C. Section 1734 solely to indicate this fact.

side: the vitreous was completely removed from the lens and the entire ciliary body was carefully separated from the sclera by microdissection. All dissections and experiments were completed within 2 h after the death of the animal.

For the manual stretching protocols that were used for the surface determination experiments, the stromal side of the iris-ciliary body (ICB) was attached with cyanoacrylate glue to a rubber washer so that the lens was suspended within the opening of the washer, which was in turn pulled by eight hooks attached to its outer prepierced edge. The washer with the glued ICB-zonulae-lens complex was then placed horizontally on an aluminum platform of a custom-built stretching device, in which experiments simulating accommodation (lens zonules relaxed) and unaccommodation (lens zonules stretched) were performed under a modified Tyrode solution (composition given in Ref. 5). Prior to the gluing, we confirmed that the center of the rubber washer remained perfectly circular when stretched and thus assured that the force separating the ciliary body from the lens would be uniformly transmitted by the zonulae, as occurs naturally in accommodation. Cow lenses looked clear, could easily be deformed, and showed no signs of abnormalities.

For experiments assessing the rapidity of the in vitro accommodation model, the aqueous side of the ICB of both bovine and rabbit specimens were affixed to the washer. The rabbit lens experiments were done in New York at Mount Sinai School of Medicine. Adult albino rabbits of either sex weighing 3–4 kg were rapidly killed by CO_2 asphyxiation, a protocol approved by the Mount Sinai Hospital Animal Care and Use Committee. After eyeballs were enucleated, a different microdissection technique than that used with the cow eye was applied owing to the more fragile nature of the rabbit ICB-lens complex. First, most of the cornea was removed via a circular cut 1–2 mm anterior to the limbal region. The attachment between the sclera and the iris base was then isolated circumferentially. Afterward, the detached sclera was removed, leaving the underlining tissues exposed. To obtain the entire ICB-zonulae-lens complex, a circular cut around the equator of the retina isolated the anterior half of the eyeball, and the vitreous was removed. The aqueous side of the ciliary body ring was attached, with a minimal amount of cyanoacrylate glue, to a rubber washer that was prepositioned within the stretching device; the washer had a central opening within which the lens was situated.

Total iridectomy was carried out on all lens complexes of both species for clear visualization of the lens margin. Tyrode solution was then added into the container with the lens to nourish the preparation.

Experimental Protocol for Manual Stretching Experiments in Cows

Bovine lenses were temporarily exposed to air for mechanical measurements and for photographing each of the two imposed accommodative states. The mechanical measurements consisted of determining the equatorial diameter (ED) in metric units by placing, from a series of plastic (acetal copolymer) washers, the washer that corresponded to the closest fit around the equator of the bovine lens in each condition. The internal diameters of such washers were precisely milled to quantify the ED. A second mechanical measurement involved determining the A-P thickness with a vernier caliper with a resolution within 0.1 mm.

For photographs, the visual axis of the camera was on the equatorial plane, perpendicular to the A-P axis of the ocular lens. Camera alignments for taking the photographs were described in detail in our reply to the Letter to the Editor of our previous lens accommodation article (4).

Determination of Lens Surface from Lateral (Sagittal) Photographs

For this determination we applied the first theorem of Pappus, which states, "the surface area S of a surface of revolution generated by the revolution of a curve about an external axis is equal to the product of the arc length of the generating curve and the distance traveled by the curve's geometric centroid." Let's clarify this concept. The center of mass of a straight line (CM_L) is a point on the line that separates the line into two equal lengths. If we progressively bend both ends of that line in the same direction, the CM_L will be displaced from the line toward the direction in which the line is curved; thus we obtain the center of mass of the curve (CM_C), which is no longer on the line. An example of how to determine the CM_C of the curve delineating the right half of the perimeter without resorting to software programs is shown in Fig. 1. The procedure is as follows: *1*) The perimeter (P) of the sagittal view of a lens (anterior side upward) is divided by the A-P axis (i.e., *line A–E* in Fig. 1), so that the right side is symmetrical to its left side; *2*) the perimeter of the whole lens is determined; *3*) that number is divided by 8; *4*) 8 points are marked clockwise on the perimeter, starting with *point A* at the anterior point of the A-P axis and finishing with *point H*, left of *point A*; *5*) *point B* is joined with *point D* and *point C* is joined with *point G*, by straight lines. The intersection of these two lines is the CM_C of the right-side curve. Similarly, the intersection of *H–F* with *C–G* determines the CM_C of the symmetrical left half. The distance between both CM_Cs is d_C, the diameter of the circle that the centroid travels in the horizontal plane.

In practice, after the lateral photographs were processed with commercial graphics software (Photoshop), we utilized the ImageJ program (procured from http://rsb.info.nih.gov/ij) to obtain the parameters, in pixels, needed to calculate the surface of the lens capsule. Furthermore, the resulting values were corroborated with the manual method described above.

Processing and Analysis of Sagittal Photographs of Bovine and Human Lenses.

The photograph in digital format was first processed in Photoshop. Afterward, the image was analyzed in ImageJ to obtain the CM_C and half the perimeter of the sagittal photograph of the lens (P_L). New lenses, as well as digital images of lenses from our previous studies (10), were used for the surface calculations presented herein. In addition, we calculated the volume of the new lenses as described previously,

$$\text{Volume of lens} = \text{CSA} \cdot \pi \cdot d \qquad (1)$$

where CSA is the cross-sectional area of half of the lens lateral profile divided by the A-P axis; and d is the diameter of the circle that crosses the center of masses of the cross-sectional areas, perpendicularly to the A-P axis (see Fig. 2 of Ref. 10). This is the second Pappus centroid theorem.

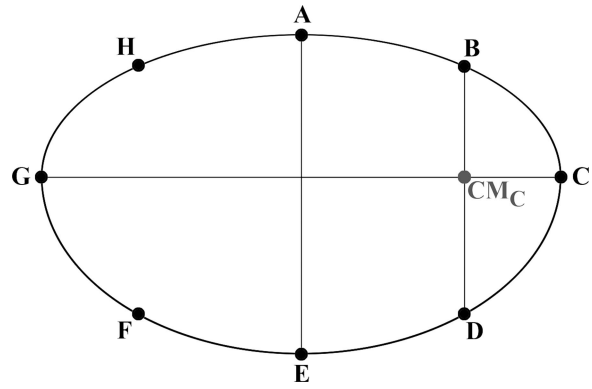

Fig. 1. Diagram for manual calculation of the center of mass of the curve between *points A* and *E*. CM_C, center of mass of the curve. See description in the text.

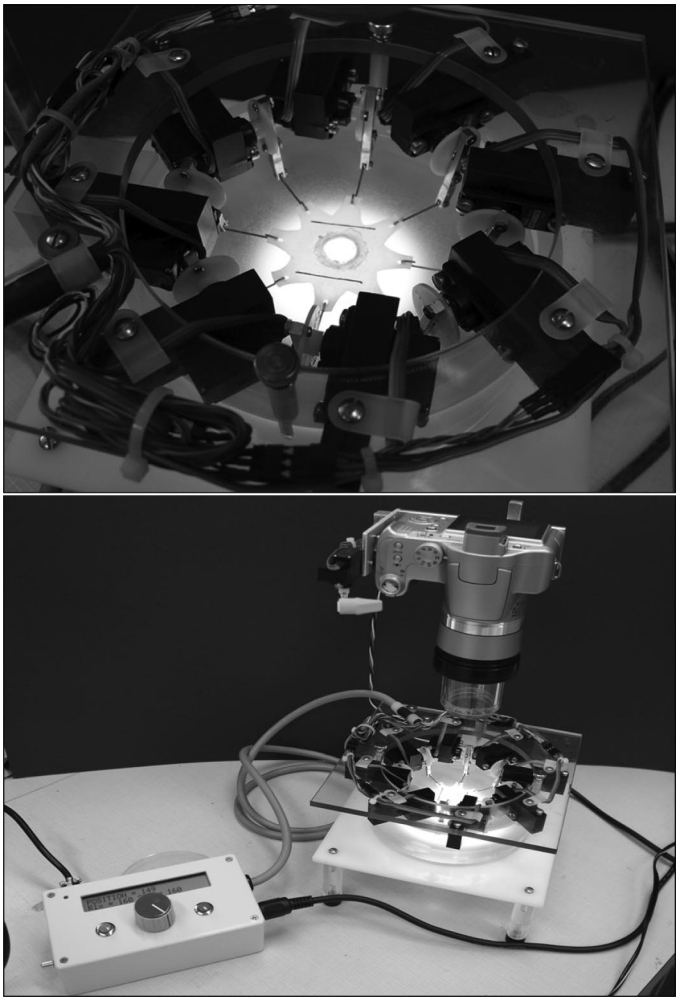

Fig. 2. Photographs of custom-built automated stretching device. *Top*: close-up of 8 servomotors, the arms of which were coordinated to simultaneously produce an evenly distributed stretching tension on a medical-grade 97% latex rubber diaphragm to which a central hole for containing the lens was cut. The ciliary body of the lens-ciliary body complex was glued on the latex. The arms of the motors could rotate back to zero tension on the diaphragm within 50 ms. *Bottom*: photograph of the camera on the gliding rail above the bathing chamber. The camera was triggered to photograph the anterior surface of the lens as described in the text.

To calculate the surface, we applied the first Pappus centroid theorem,

$$\text{Surface of lens} = P_L \cdot \pi \cdot d_C \quad (2)$$

where P_L = half the perimeter of the sagittal photograph of the lens; and $d_C = 2CM_C$.

The steps carried out for attaining the parameters needed for calculating the above-mentioned formulas were as follows.

Using Photoshop. The ellipse tool was chosen to delineate a figure that fit as close as possible around the outline of the lens.

Since the anterior and posterior surfaces of the lens are not symmetrical, it was necessary to use the warp tool to contour this ellipse around the lens edges.

The maximum distance between the two bow zones, perpendicular to the A-P axis (i.e., the equatorial length), was obtained in pixels. At exactly the midpoint of the equator, which comprises the intersect with the A-P axis, half of the whole lens CSA was selected, copied, and pasted somewhere else in the picture, using the Selection tool.

From the CSA of half of the lens, its curve was obtained utilizing the Magic Wand tool.

The processed figure contained the whole cross-sectional outline of the lens, the CSA of half of the lens and the curve of the latter.

Using ImageJ. Using the Wand (tracing) tool, the boundaries of the curve and the outline of the half lens and the whole lens were demarcated. The measurements (in pixels) in the "analyze" pull-down menu yielded CM_C, d_C, ED, and P_L.

To validate that the lens half (obtained in Photoshop) was exactly half of the whole lens figure, twice the CSA and twice P_L had to be within 0.5% of the cross-sectional area and perimeter of the whole lens, respectively. If not, the original lens picture was reprocessed in Photoshop until the parameters of the figures fell within the 0.5% error difference that was chosen as acceptable.

Next, the pixels obtained on ImageJ were converted to centimeters by first establishing the ratio between the equator, in pixels, and a known plastic washer, in centimeters. For example, 252.2 pixels equals 1.79 cm for *lens A* in Table 2; therefore, the ratio is 140.9 pixels/cm. All remaining ImageJ determinations, in pixels, were converted to metric units in comparable fashion, and further applied to *Eqs. 1* and *2* to obtain lens surfaces and volumes in both accommodative states.

Similarly, models of human lenses 20 yr old (0 and 10 D of accommodation) and 45 yr old (0 and 4 D of accommodation) were analyzed for surface changes, following the aforementioned steps. The description of the construction of these lenses, from data obtained in the scientific literature, was described elsewhere (4, 10).

Determination of Rate of Equatorial Diameter Recovery

Previously, we showed that stretching or increasing lens ED results in a loss of volume (10). Present experiments to determine the rate of recovery of cow and rabbit lens ED following a sudden relaxation from sustained stretching were performed with a custom-built apparatus. The apparatus was composed of three major components (Fig. 2): *1*) a circular water bath to which an upwardly pointing gliding rail was fastened to form the base of the apparatus; *2*) a mount that fixed a digital camera in place and connected it to the gliding rail; and *3*) a lens-complex stretching device. The stretching device was the most intricate component and contained eight motors evenly mounted on a circular module. These motors were synchronized to simulate unaccommodation and accommodation by respectively transmitting radial stretching forces and relaxation to the ICB-zonulae-lens complex via eight metal hooks clasping the prepierced outer edge of the rubber washer shown in Fig. 2. The motors were preprogrammed to coordinate their motion with the controller of the camera shutter so that pictures could be taken with a predetermined time delay respective to the motors' activity; i.e., 200 ms and 5 s following release of the radial stretching force. The apparatuses used for rabbit and bovine lenses differed only in the operating range of their stretching and relaxation actions owing to the differences in the sizes of the lenses from the two species. The digital camera was aligned as needed along the gliding rail and positioned with a custom-built adaptor to the camera lens that enabled immersion into the Tyrode solution without touching the ocular lens.

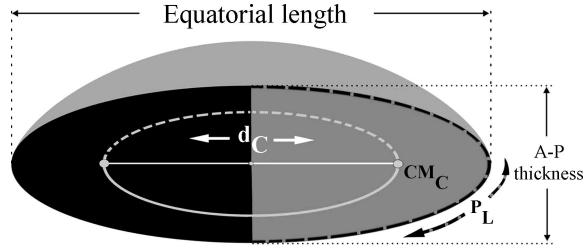

Fig. 3. Diagram showing the parameters necessary to calculate the surface of the lens. P_L, half the perimeter of the sagittal photographs of the lens; A-P, anterior-posterior; d_C, diameter of the circle that the centroid travels in the horizontal plane.

Table 1. *Changes in parameters of 20- and 45-yr-old models of human lenses during accommodation*

	ED, cm	A-P Thickness, cm	P_L, cm	CM_C, cm	Surface, cm^2	Volume, cm^3
20-yr-old						
10 D	0.90	0.42	1.10	0.25	1.72	0.155
0 D	0.92	0.37	1.10	0.25	1.72	0.151
% Difference	2.22	−11.90	0.00	0.00	0.00*	−2.58
45-yr-old						
4 D	0.93	0.45	1.16	0.26	1.89	0.183
0 D	0.94	0.44	1.17	0.26	1.92	0.180
% Difference	1.07	−2.22	0.86	0.00	1.59	−1.64

*Theoretically these should be a small increase, which was not detected by the resolution of our method. A-P, anterior-posterior; P_L, half the perimeter of the sagittal photographs of the lens; CM_C, center of mass of the curve; D, diopter; ED, equatorial diameter.

The visual axis of the camera was centered in line with the A-P axis of the ocular lens, so that pictures of the entire anterior surface were captured. As a reference point, the camera focus was adjusted manually until a clear image of the ciliary process could be seen. The shutter speed was fixed at 1/250 s in all experiments.

In every experiment, three to four sets of digital photos in the following sequence were taken: *1*) the baseline situation with a relaxed ocular lens; *2*) after the imposition of a stretched ocular lens; *3*) 200 ms following release of the stretching force; and *4*) 5 s after the stretching force was released. The stretching intensity was set to a low arbitrary value for the first set of pictures. Afterward, the intensity was increased sequentially and new sets of pictures were taken at each step. The final chosen set analyzed was the one matching a desired increase in lens diameter (typically an increase in ED of ~3%) as described below.

Digital images of the crystalline lenses were processed with graphic software (Photoshop). The images were first assessed for deformation, set-by-set from low to high stretching intensity. A lens was considered deformed if there was a notable irregularity or a larger than 4% difference between its longest and shortest lens diameters. A deformation indicated either a break of the gluing due to the stretching force applied, or simply a poor attachment. Picture sets passing this preliminary test were further analyzed. The average of the longest and shortest diameters of a lens in the baseline condition was compared with that of the stretch-sustained and the two stretch-released conditions thereafter. In control experiments the rubber washer was stretched without the lens and it was determined that it reverted to its relaxed state in less than 200 ms, after the force was released.

Since all the mechanical and photographic settings remained constant between photographs, comparisons of equatorial pixels gives the changes in equatorial diameter of the lens between the relaxed and stretched conditions without need to convert to metric units. Nevertheless, we recorded the equatorial diameter of the relaxed lenses using the plastic washer as previously described for the measurement of cow lens surface. In general, the equatorial diameter of the lenses used for this part of the study were within the range of lenses in which the volume and surface area were determined.

RESULTS

Surface in the Human Model

The same model of the human lens that was used to determine volume changes in our previous work (10) is shown in Fig. 3, but with the additions of CM_C and P_L to calculate the surface. Measured and calculated parameters from this model are compiled in Table 1. For the modeled lenses in the relaxed and stretched conditions the perimeter was maintained constant, a condition we imposed in our analysis but one that may not necessarily represent the in vivo situation. Yet, under this situation, CM_C separates from a line that divides the lens into two halves, and as a consequence the surface increases. This can be easily visualized if one totally flattens a sphere, transforming it into two disks. The surface area of the two disks will be ~25% larger than that of the original sphere. For the 20-yr-old human lens model (Table 1), there was no change in surface as the lens unaccommodates (10 D to 0 D) and the volume decreases. For the 45-yr-old lens model, the unaccommodation from 4 D to 0 D yielded 1.6% increase in surface (Table 1).

Surface in the In Vitro Cow Lens

These results are shown in Tables 2 and 3. In addition to the expected increase in ED and decrease in A-P with stretching, a striking finding was the decrease P_L in four of the six lenses (excluding *lenses C* and *F*) in Table 2, and all lenses in Table 3. This decrease, of course, will affect the value of the surface. Nevertheless, the volume decreased in all lenses, except one. Furthermore, in some cases there was a decrease in surface with stretching, whereas in others there was an increase. These changes are consistent with changes in CM_C, P_L, or both. In the case where there was a decrease in surface, the change coincided, in most lenses, with a change in equator length of 0.4 mm or less. In those lenses in which the total surface increased with stretching, the increase in equator length was as high as 0.6 mm.

Velocity of Relaxation

In these experiments, we used a software-driven apparatus synchronized with a digital camera. With controlled stretching

Table 2. *Measurements of bovine lenses in Tyrode solution*

	ED, cm		Difference in ED, mm	A-P thickness, cm		P_L, cm		CM_C, cm		Surface Total, cm^2		Volume, cm^3	
Lens	Relaxed	Stretched		Relaxed	Stretched	Relaxed	Stretched	Relaxed	Stretched	Relaxed	Stretched	Relaxed	Stretched
A	1.79	1.82	0.3	1.29	1.24	2.59	2.53	0.56	0.53	9.11	8.43	2.16	2.03
B	1.65	1.68	0.3	1.21	1.14	2.41	2.32	0.51	0.49	7.72	7.14	1.73	1.55
C	1.85	1.91	0.6	1.31	1.30	2.62	2.63	0.57	0.57	9.38	9.42	2.24	2.25
D	1.65	1.71	0.6	1.25	1.19	2.43	2.40	0.51	0.52	7.79	7.84	1.75	1.71
E	1.79	1.83	0.4	1.23	1.18	2.51	2.50	0.53	0.53	8.36	8.33	1.99	1.93
F	1.82	1.86	0.4	1.27	1.27	2.57	2.58	0.56	0.56	9.04	9.08	2.20	2.18
Mean	1.758	1.802		1.260	1.219	2.522	2.494	0.538	0.536	8.567	8.373	2.013	1.941
SE	0.035	0.036		0.016	0.025	0.036	0.047	0.011	0.012	0.291	0.337	0.092	0.111
% Diff of mean		2.503			−3.254		−1.110		−0.372		−2.265*		−3.577†

*Statistically not significant, $P > 0.2$. †Statistically significant, $P < 0.05$.

Table 3. *Measurements of bovine lenses in oil*

Lens	ED, cm		Difference in ED, mm	A-P Thickness, cm		P_L, cm		CM_C, cm		Surface Total, cm^2		Volume, cm^3	
	Relaxed	Stretched		Relaxed	Stretched	Relaxed	Stretched	Relaxed	Stretched	Relaxed	Stretched	Relaxed	Stretched
1	1.69	1.72	0.3	1.22	1.16	2.40	2.37	0.57	0.51	8.60	7.59	1.75	1.66
2	1.62	1.65	0.3	1.17	1.13	2.32	2.30	0.50	0.50	7.29	7.23	1.58	1.53
3	1.68	1.71	0.3	1.18	1.13	2.38	2.32	0.51	0.50	7.63	7.29	1.71	1.49
4	1.75	1.75	0.0	1.23	1.16	2.48	2.37	0.53	0.52	8.26	7.74	1.93	1.60
6	1.79	1.79	0.0	1.23	1.17	2.49	2.42	0.53	0.52	8.29	7.91	1.93	1.77
7	1.77	1.79	0.2	1.20	1.14	2.44	2.38	0.52	0.51	7.97	7.63	1.83	1.65
Mean	1.717	1.735		1.204	1.147	2.415	2.359	0.527	0.510	8.007	7.565	1.788	1.615
SE	0.026	0.022		0.010	0.006	0.026	0.018	0.010	0.004	0.196	0.107	0.056	0.041
% Diff of mean		1.048			−4.734		−2.319		−3.226		−5.520†		−9.676*

Statistically significant, †$P < 0.02$; *$P < 0.01$.

of the lens, we induced an increase of the ED of ~3%, which was the change corresponding to a volume decrease of 5–6% as previously determined (10). The stretching force that flattened the lens was sustained for ~3 s. After anterior face of the lens was photographed, the stretching force was suddenly released and the software directed the camera to take pictures 200 ms and 5 s later. These pictures were compared with the control picture taken before the lens was stretched. It was found that after 200 ms of the stretching force release, the increased ED recovered 90% of its original value, in the cow, whereas the rabbit lens restored 98% of its ED. Five seconds later, ED completely regained its control length on both species. These results are summarized in Tables 4 and 5.

DISCUSSION

The purpose of these experiments was *1*) to find a method to measure lens surface and its possible change during accommodation, and *2*) to measure the time necessary for a lens to revert from its stretched ED in vitro, which represents a lens volume increase (10).

Classical interpretations of lens accommodation that date to the 19th century suggest that lens volume is constant during accommodation and implicitly assume that only the surface must change (13), although changes in these parameters were never measured previous to our recent publication on volume changes. On the basis of the physical fact that the surface of an ellipsoid increases as it gets flatter, we predicted (10) that simultaneously with the decrease in volume, the surface of the lens should increase around the equator. That was the case for the analysis of the human lens model presented herein. An increase in surface of 1.6 percent was associated with the volume decrease (unaccommodation) in the 45-yr-old human lens with 4 D of accommodation. A change in surface was not detected by our method in the 20-yr-old human lens model with 10 D of accommodation, which does not necessarily mean that the surface remains constant. It is possible that changes in the equatorial area are compensated by opposite changes in another area of the lens. Furthermore, imposing a restriction of constant perimeter of the sagittal outline of the model lens (as we elected for simplicity) prevents changes of the lens surface around the poles.

In extensive and elegant studies, Kuszak et al. (16) demonstrated species differences in lenticular fiber structure (particularly at the sutures). These authors concluded that in primates (including humans), lens accommodation occurs with a controlled realignment of the flattened fiber ends along multiple suture levels throughout the anterior and posterior surfaces. Kuszack et al. also reasoned that lenses of species such as cow

Table 4. *Changes in equatorial lens diameter upon simulated accommodative changes in in vitro bovine lens preparations*

Lens	ED, pixels			
	Relaxed Control	Stretched	200 ms After Relaxation	5 s After Relaxation
A	5,340.0	5,469.0	5,368.0	5,350.5
B	4,906.0	5,083.5	4,916.5	4,909.5
C	4,906.5	4,996.5	4,923.5	4,910.0
D	4,701.5	4,823.0	4,719.0	4,698.0
E	4,798.5	4,993.0	4,795.0	4,795.0
F	4,719.0	4,826.5	4,733.0	4,719.0
G	4,895.5	4,982.5	4,895.5	4,889.0
H	4,736.0	4,847.0	4,750.0	4,746.5
I	4,993.0	5,142.5	5,007.0	4,993.0
Mean	4,888.4	5,018.2*	4,900.8†	4,890.1
SE	65.7	67.6	67.2	66.6
% Change from control		+2.7	+0.3	0.0

Statistically different from relaxed control, as paired data: *$P < 0.001$; †$P < 0.01$.

Table 5. *Changes in equatorial lens diameter upon simulated accommodative changes in in vitro rabbit lens preparations*

Lens	ED, pixels			
	Relaxed Control	Stretched	200 ms After Relaxation	5 s After Relaxation
J	3,770.5	3,858.0	3,789.0	3,789.0
K	4,316.0	4,413.5	4,328.5	4,321.0
L	4,305.5	4,407.5	4,294.0	4,290.0
M	4,358.5	4,477.5	4,347.0	4,341.5
N	3,826.5	3,920.5	3,826.5	3,824.0
O	3,920.5	4,037.0	3,943.0	3,923.0
P	3,963.0	4,078.0	3,960.5	3,955.5
Q	4,012.5	4,141.5	4,012.5	4,005.0
R	3,984.0	4,097.0	3,988.0	3,984.5
Mean	4,050.8	4,158.9*	4,053.4	4,048.2
SE	73.5	74.6	71.5	71.4
% Change from control		+2.7	+0.1	−0.1

*Statistically significant with respect to relaxed control, $P < 0.01$.

(which possess a Y-shaped suture) and rabbit (which possess a line suture) have very limited accommodative range, at least partially because of the shape of their fiber ends, which do not allow overlapping.

However, our experiments using in vitro cow lenses were not intended to directly model human accommodation. We merely aimed to deform the lens using radial forces similar to natural accommodation and quantify the changes in volume and surface that occurred, a subject heretofore unexplored. Our data illustrate the only manner in which a lens shape could change regardless of whether it occurred as a result of a natural or artificial deformation. Accommodative powers of bovine and rabbit eyes have not been determined; however, it was suggested that these species could attain an accommodation of ~2 D (1, 19). Our earlier results are generally in accord with this view (10). In that work we measured the radii of curvature of the bovine lens from lateral photographs and calculated the equivalent dioptric change in two extreme accommodative states.

More recently, we shone a single point light through the bovine lens, in both relaxed and stretched states, and measured the changes in focal length on a screen. Our results (unpublished data) were consistent with the calculated dioptric powers from the change of radii of curvatures. We concluded from these experiments that increasing ED by ~2% induces an equivalent unaccommodation of ~2 D, which occurs concomitantly with a decrease in volume of between 4 and 10% (10).

Furthermore, we found that in most lenses in which the stretching force increased the ED 0.4 mm or less (except on *lens E* of Table 2), the total surface of the lens decreased. This equatorial change seems to be the point of stretching at which the surface starts to increase. The reversal in surface change can be explained if one assumes that when the lens is maximally rounded the capsule covering the anterior polar region is somewhat under tension and stretched by the disposition of the internal lens fibers while the capsule around the equator area is relaxed. As a stretching force is exerted around the equator, the lens deforms with a release of the polar tension and a decrease in A-P distance, with little increase in ED. This results in an initial decrease in lens surface in the polar area. The idea that a collapse occurs at the anterior pole is based in the determination that most of the curvature change during accommodation is on the anterior aspect. As the stretching force is further increased, ED and the equatorial circumference increase as well. By necessity, this change creates additional surface between the insertion area of the zonulae in the lens capsule that separates from the center of lens. At a point, the total area of the lens surface changes from a decrease to an increase. The initial collapse of the polar region can quickly change the curvature of the anterior face and facilitate focusing of distant objects; Pedrigi et al. (18) and David et al. (8) provided evidence for differences in regional elasticity of the capsule, suggesting that our interpretations may be valid.

The rapid changes observed in bovine and rabbit lens ED during our experiments imply that the displacement of volume previously observed (10) can occur within a physiologically relevant time frame. Although it was not our intention to compare the speed of "shape recovery" of cow and rabbit lenses with human lenses, it is interesting to note that our in vitro results generally agree with the speed of in vivo accommodation determined in human by Kasthurirangan and Glasser (15). Thus we have showed that the lens can regain its volume in vitro in ~200 ms, also implying that the lens can lose a similar volume during unaccommodation.

GRANTS

This research was supported by National Eye Institute Grants EY-000160 and EY-001867 and by RPB, Inc.

REFERENCES

1. **Bettelheim FA.** Syneretic response to pressure in ocular lens. *J Theor Biol* 197: 277–280, 1999.
2. **Brown N.** The change in shape and internal form of the lens of the eye on accommodation. *Exp Eye Res* 15: 441–459, 1973.
3. **Burd HJ, Judge SJ, Cross JA.** Numerical modelling of the accommodating lens. *Vision Res* 42: 2235–2251, 2002.
4. **Candia OA.** Reply to "Letter to the editor: 'Ocular lens does not change volume during accommodation.'" *Am J Physiol Cell Physiol* 293: C1729–C1730, 2007.
5. **Candia OA, Alvarez LJ, Zamudio AC.** Regulation of water permeability in rabbit conjunctival epithelium by anisotonic conditions. *Am J Physiol Cell Physiol* 290: C1168–C1178, 2006.
6. **Croft MA, Glasser A, Kaufman PL.** Accommodation and presbyopia. *Int Ophthalmol Clin* 41: 33–46, 2001.
7. **Cruz-Orive LM, Roberts N.** Unbiased volume estimation with coaxial sections: an application to the human bladder. *J Microsc* 170: 25–33, 1993.
8. **David G, Pedrigi RM, Heistand MR, Humphrey JD.** Regional multiaxial mechanical properties of the porcine anterior lens capsule. *J Biomech Eng* 129: 97–104, 2007.
9. **Dubbelman M, van der Heijde RG, Weeber HA.** Comment on "Scheimpflug and high-resolution magnetic resonance imaging of the anterior segment: a comparative study." *J Opt Soc Am A Opt Image Sci Vis* 22: 1216–1218; discussion 1219–1220, 2005.
10. **Gerometta R, Zamudio AC, Escobar DP, Candia OA.** Volume change of the ocular lens during accommodation. *Am J Physiol Cell Physiol* 293: C797–C804, 2007.
11. **Gillum W.** Mechanisms of accommodation in vertebrates. *Ophthalmic Semin* 1: 253–286, 1976.
12. **Glasser A, Croft MA, Kaufman PL.** Aging of the human crystalline lens and presbyopia. *Int Ophthalmol Clin* 41: 1–15, 2001.
13. **Gullstrand A.** How I found the mechanism of intracapsular accommodation. In: *Nobel Lectures, Physiology or Medicine 1901–1921*. Amsterdam: Elsevier, 1967, p. 414.
14. **Kasprzak HT.** New approximation for the whole profile of the human crystalline lens. *Ophthalmic Physiol Opt* 20: 31–43, 2000.
15. **Kasthurirangan S, Glasser A.** Age related changes in accommodative dynamics in humans. *Vision Res* 46: 1507–1519, 2006.
16. **Kuszak JR, Mazurkiewicz M, Jison L, Madurski A, Ngando A, Zoltoski RK.** Quantitative analysis of animal model lens anatomy: accommodative range is related to fiber structure and organization. *Vet Ophthalmol* 9: 266–280, 2006.
17. **Mironov AA Jr, Mironov AA.** Estimation of subcellular organelle volume from ultrathin sections through centrioles with a discretized version of the vertical rotator. *J Microsc* 192: 29–36, 1998.
18. **Pedrigi RM, David G, Dziezyc J, Humphrey JD.** Regional mechanical properties and stress analysis of the human anterior lens capsule. *Vision Res* 47: 1781–1789, 2007.
19. **Rafferty NS, Scholz DL.** Comparative study of actin filament patterns in lens epithelial cells. Are these determined by the mechanisms of lens accommodation? *Curr Eye Res* 8: 569–579, 1989.
20. **Reed MG, Shanks E, Beech DJ, Barlow L, Howard CV.** Stereological estimation of eye volume using the Pappus method. *J Microsc* 202: 473–479, 2001.
21. **Rosen AM, Denham DB, Fernandez V, Borja D, Ho A, Manns F, Parel JM, Augusteyn RC.** In vitro dimensions and curvatures of human lenses. *Vision Res* 46: 1002–1009, 2006.
22. **Schachar RA, Huang T, Huang X.** Mathematic proof of Schachar's hypothesis of accommodation. *Ann Ophthalmol* 25: 5–9, 1993.
23. **Stewart WJ, Rodkey SM, Gunawardena S, White RD, Luvisi B, Klein AL, Salcedo E.** Left ventricular volume calculation with integrated backscatter from echocardiography. *J Am Soc Echocardiogr* 6: 553–563, 1993.
24. **Strenk SA, Strenk LM, Semmlow JL, DeMarco JK.** Magnetic resonance imaging study of the effects of age and accommodation on the human lens cross-sectional area. *Invest Ophthalmol Vis Sci* 45: 539–545, 2004.